



Antimicrobial activity of chitosan against biofilm formation of klebsiella pneumonia and staphylococcus aureus associated with burn infections

Zaedoon Monaam*, Mayada Al-khafaji

Department of Medical Lab. Techniques, College of Health and Medical Techniques, Gilgamesh University, Baghdad, Iraq

*) Email: zaidoun.monaam1206a@sc.uobaghdad.edu.iq

Received 23/10/2024, Received in revised form 17/11/2024, Accepted 19/11/2024, Published 15/2/2025

The effect of chitosan on the biofilm-forming capacity of clinically isolated bacteria was investigated in this study. Chitosan (Biopolymer from Chitin) was made through a series of tests. Patients at Baghdad Medical City Hospital provided 133 clinically burn swap samples. According to the Vitik 2 test, *Staphylococcus aureus* was detected in 19 of them and *Klebsiella pneumonia* in 70 of them. Five *S. aureus* and twenty-five *Klebsiella pneumonia* were able to generate biofilm when cultivated in microtiter plates. According to the results, chitosan was more successful at stopping the formation of biofilm at a dosage of 1.6 mg/ml. These results imply that this drug may be used to treat Multidrug resistance bacteria (MDR) in the future.

Keywords: Antimicrobial activity; Chitosan; Biofilm formation; Klebsiella pneumonia.

1. INTRODUCTION

Acute and chronic infections often involve multidrug-resistant (MDR) strains like *Staphylococcus aureus* and *Klebsiella pneumoniae*, which lead to significant morbidity, mortality, and increased healthcare costs. Significant research has revealed a connection between bacterial biofilms and human illnesses. Biofilms, which are clusters of bacteria encased in a self-produced extracellular matrix, enhance bacterial resistance to antibiotics and immune defenses by fostering growth on surfaces. This biofilm formation alters the bacteria's metabolic functions and genetic activity, making them harder to eliminate [1]. Biofilms are common among various pathogens and hospital-acquired bacteria in both natural environments and infected tissues, playing a crucial role in chronic human infections [2]. The second most abundant polymer on Earth, chitin is a naturally occurring polymer made up of β -(1-4)-

poly-N-acetyl-D-glucosamine and is frequently found in the exoskeletons of insects, shrimp, crabs, and lobsters. By removing the acetyl group (CH₃-CO) from chitin, poly-(β-1!4)-2-amino-2-deoxy-D-glucopyranose is created, which is then converted into chitosan [3]. The extraction of chitosan from shellfish involves removing minerals and proteins, which can be done using either chemical or enzymatic methods. Chitosan is renowned for its low toxicity, biodegradability, and biocompatibility, making it useful in various applications, including water treatment as a flocculant, as an elicitor in plant defense mechanisms, and in food preservation and additives. It also serves as a drug delivery vehicle, hydrogel film in pharmaceuticals, and dehydrating agent in cosmetics [4]. Nanotechnology, which involves manipulating matter at the molecular and atomic scale, has revolutionized various fields, including medicine. In the context of antimicrobial treatments, nanomaterials have shown great promise in combating multidrug-resistant (MDR) pathogens and biofilm formation [5]. Nanoparticles such as silver, copper, and chitosan-based nanocomposites are being explored for their ability to inhibit biofilm development, which is a major challenge in treating chronic infections. These nanomaterials can interact with bacterial cells at the nanoscale, enhancing their antimicrobial properties and offering a new avenue for tackling resistant infections. The integration of nanotechnology into drug delivery systems, such as chitosan nanoparticles, could enhance the therapeutic efficacy of traditional antibiotics, particularly in cases where biofilms impair the effectiveness of standard treatments [6]. Chitosan exhibits antibacterial and antifungal properties, as reported in numerous studies. The molecular weight (MW) and distribution of deacetylated chitosan are influenced by demineralization and deproteinization processes. For example, prolonged elevated-temperature de-proteinization results in lower molecular-weight of chitosan that deacetylated. The anti-biofilm efficacy of chitosan varies depending on the target microorganism and is partly due to its physicochemical characteristics.

2. METHODOLOGY USED

2.1 Isolation and Identification

From October 1, 2023, to December 20, 2023, 154 burn samples (swabs) were collected from patients at the Medical City Hospitals in Baghdad (burn center) to detect pathogenic bacteria. Initially, the swabs were cultured in Brain Heart Infusion (BHI) broth and incubated at 37°C for 24 hours. After incubation, the samples were transferred onto blood agar and MacConkey agar plates. Distinct colonies were then isolated based on their morphological characteristics and subsequently subculture on nutrient agar slants for further analysis [7].

2.2 Nanochitosan Preparation and Characterization

To enhance the efficacy of chitosan, nanochitosan particles were prepared through ionic gelation techniques using sodium tripolyphosphate (TPP) as a cross-linking agent [8]. Chitosan was dissolved in 1% acetic acid solution, and TPP was added dropwise under continuous stirring to form nanoparticles. The resulting nanochitosan was characterized using dynamic light scattering (DLS) to determine particle size and zeta potential, ensuring optimal size distribution for enhanced antimicrobial activity [6].

2.3 Isolation of *Staphylococcus aureus*.

Samples that exhibited growth on blood agar but not on MacConkey agar were subjected to Gram staining. Gram-positive colonies were then tested with the catalase test, which returned positive results. These colonies were subsequently cultured on Mannitol Salt Agar (MSA), a medium both selective and differential for staphylococci. Colonies that fermented mannitol were selected for the coagulase test using 10% rabbit plasma. Samples that tested positive in the coagulase test were confirmed as *Staphylococcus aureus* [9].

2.4 Isolation of *Klebsiella Pneumonia*

Samples that exhibited growth on both blood and MacConkey agar, specifically those with lactose-fermenting colonies, were collected and subjected to Gram staining. The Gram-negative colonies were then inoculated into Triple Sugar Iron (TSI) agar slants, resulting in an acid/acid gas reaction.; colonies were subjected to a catalase test, and those showed positive results with no green metallic sheen on EMB agar were primarily considered as *K. pneumonia* [10].

2.5 Antibiotic Susceptibility Testing

The dehydrated Mueller-Hinton agar was reconstituted according to the manufacturer's directions. Before the medium was put into petri dishes, it was chilled to -20°C. To allow the agar to solidify, the plates were then placed upright with their lids tilted and placed in an incubator set at 35°C for 30 minutes. The inoculum was prepared by transferring three to five bacterial colonies into a tube containing five milliliters of normal saline (0.85% NaCl), vigorously mixing the mixture, and adjusting the turbidity to match a McFarland standard. This resulted in a concentration of 1.5×10^8 CFU/ml, which is equal to McFarland 0.5. Thirty minutes after preparation, these suspensions were put to use. A sterile brush was dipped into the bacterial suspension and rotated and pressed against the tube's inner wall to remove any surplus liquid before inoculating the plates. Using forceps, a few antibiotic discs were chosen and placed on the inoculation plates in accordance with CLSI M100 2020 recommendations. Four to five discs were placed gently on the agar surface after being pre-warmed to room temperature in each plate. After that, the infected plates were incubated inverted for the entire night at 37 °C [11, 17].

2.6 Quantitative Formation Assay of Biofilm

The production of biofilms in pathogenic isolates was detected using the microliter plate method. These isolates were grown for an entire night in tryptic soy broth (TSB) with 1% glucose added as a supplement. After that, the bacterial cultures were well mixed, diluted in 5 milliliters of sterile normal saline (0.84% NaCl), and standardized to meet McFarland requirements. The experiments were then carried out in triplicate, with 20 µl of each bacterial culture applied to three wells of a polystyrene microtiter plate that each contained 8 µl of TSB with 1% glucose. For 18 to 24 hours, the plate was incubated at 37°C. Following incubation, loosely adherent cells were removed from the wells by aspirating the contents and washing them three times in PBS (pH7). An incubation period of 15 minutes at 40°C was used to secure the remaining bacterial adhesion. After that, the wells were dyed for five minutes at room temperature using 126 µl of a 0.1% crystal violet solution. To enable quantitative biofilm investigation, 95% ethanol was applied to the wells for 16 minutes after staining and they were then cleaned with PBS (pH 7). With the use of an ELISA microtiter plate reader, the absorbance of the crystal violet stain was determined at 630 nm. To account for non-specific crystal violet binding, control wells with just the culture medium and no bacteria were employed. The following formula was used to determine the adhesion of biofilm formation [12, 18].

Adherence of biofilm Formation = OD_s/OD_c

Where: OD_s = is the mean optical density at 630 nm of the bacterial samples. OD_c = is the mean optical density at 630 nm of the control samples.

2.7. Recovery and Extraction of Chitosan

The process for measuring chitosan content started by homogenizing the entire solid-state biomass with 1M NaOH at a 1:30 (w/v) ratio, followed by autoclaving at 121°C and 15 psi for 15 minutes. Alkali-insoluble materials (AIMs) were then filtered out using cotton gauze and washed with distilled water until a neutral pH was achieved. These AIMs were transferred to glass petri dishes, weighed, and then dried overnight in an oven set at 60°C. For chitosan extraction, the AIMs were treated with 2% acetic acid at a 1:40 (w/v) ratio and autoclaved for 15 minutes. The mixture was then centrifuged at 10,000 rpm for 15 minutes. The AIMs were discarded, and the pH of the supernatant was adjusted to 10 using 4M NaOH. After an overnight standing period, the mixture was centrifuged again to collect the precipitates, which were then washed and weighed. The precipitates underwent further purification using acetone at a 1:20 (w/v) ratio and 95% ethanol at a 1:20 (w/v) ratio. Finally, the chitosan precipitate was dried at 60°C and quantified as milligrams of chitosan per gram of chitin [9].

2.8 Characterizations of Chitosan

2.8.1 Quantification of Deacetylation Degree (DDA)

The Degree of Deacetylation (DDA) of chitosan was ascertained by creating a standard curve for N-acetylglucosamine (GlcNAc). A 0.1 mg/ml stock solution was used to create various concentrations of GlcNAc, including 0.01 mg/ml, 0.02 mg/ml, 0.03 mg/ml, and 0.05 mg/ml. By adding 0.1 ml of 0.001M HCl without GlcNAc, a control blank was created. The absorbance of each concentration was measured at 199 nm after a 5-minute interval. A standard curve connecting the GlcNAc concentrations (mg/ml) with corresponding absorbance readings was then plotted using this data [14, 19].

2.8.2 Fourier-Transform Infrared Spectroscopy Analysis of Chitosan

FTIR spectroscopy was used to compare samples of chitosan that were manufactured in a lab with those that were purchased commercially [14]. To achieve this, 2 mg of chitosan and 101 mg of potassium bromide (KBr) were carefully combined after being dried overnight at 60°C under low pressure. After compressing this mixture into disks that were 0.5 mm thick, it was dried for 24 hours at 110°C with low pressure. The Bruker 66 Spectrometer was used to record infrared spectra, with a 100 mg blank KBr disk serving as the reference. After that, the spectroscopic outcomes were contrasted with those of chitosan made from *Aspergillus flavus* F3 [20].

2.9 Assessment of Chitosan's Anti-Biofilm Efficacy

To evaluate chitosan's effectiveness against biofilm formation, we chose the most robust biofilm-producing strains of *Klebsiella pneumoniae* and *Staphylococcus aureus*. Each bacterial strain was tested in triplicate. Biofilm development was assessed both in the presence and absence of chitosan to observe its direct impact. Sub-inhibitory doses of chitosan were added to each bacterial culture, and the subsequent effects on biofilm formation were meticulously recorded and analyzed.

3. RESULTS AND DISCUSSION

From the 151 wound swab samples collected, 41 showed no bacterial growth, likely due to factors such as the presence of viruses or anaerobic bacteria, which were not included in this study. Biochemical tests identified 110 bacterial isolates. Among these, *Staphylococcus aureus* accounted for 22.7% (25 cases), *Klebsiella pneumoniae* for 40% (45 cases), other gram-positive bacteria for 8.6%, and gram-negative bacteria for 28.7%. The distribution of these isolates is illustrated in Figure 1.

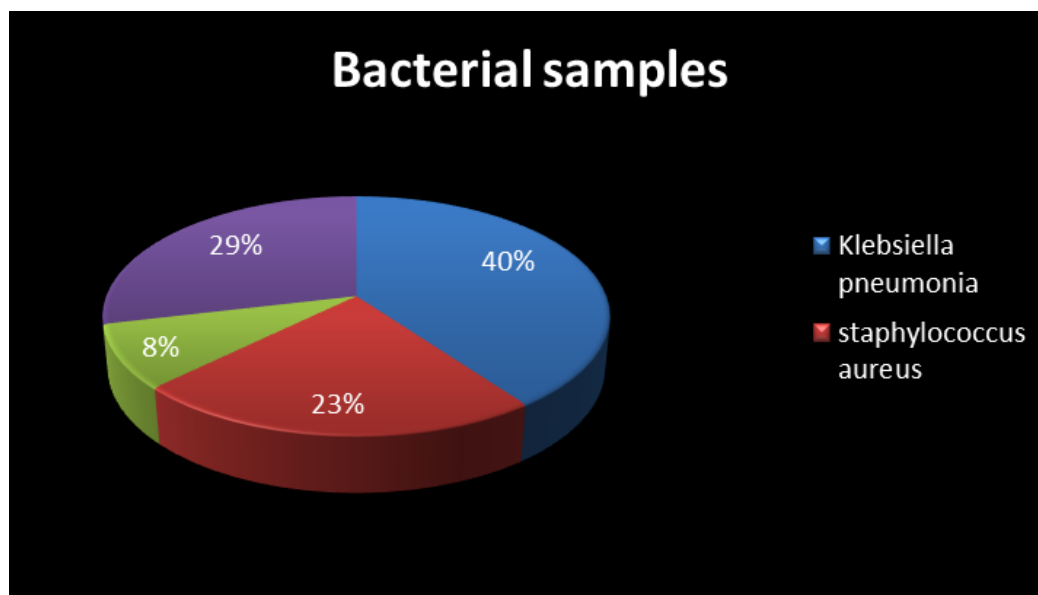


Figure 1 Rate of bacterial isolates with burn samples.

3.1 Nanochitosan's Antimicrobial Activity

Nanochitosan demonstrated significant antimicrobial activity against both *Staphylococcus aureus* and *Klebsiella pneumoniae*. The nano-scale size of the particles enhanced their ability to penetrate biofilms and disrupt bacterial cell walls [15]. This improved efficacy is attributed to the increased surface area and the enhanced interaction between the nanoparticles and bacterial cells [16].

3.2 Susceptibility Test of Bacterial Isolates

The most of bacterial isolates in this study exhibited significant antibiotic resistance. For *Staphylococcus aureus*, resistance rates were as follows: 74% to penicillin, 44% to cefepime, 100% to gentamycin, 70% to tobramycin, 31% to amikacin, 85% to levofloxacin, 52% to chloramphenicol, 63% to nitrofurantoin, and 100% to tetracycline, as shown in Figure 2 .

Klebsiella pneumoniae isolates demonstrated the following resistance rates: 85% to ceftazidime, 48% to cefepime, 78% to gentamycin, 43% to amikacin, 19% to tobramycin, 62% to levofloxacin, 60% to piperacillin, 82% to colistin, 68% to imipenem, and 61% to aztreonam, detailed in Figure (3). Antibiotic resistance is increasingly reported among clinical strains, complicating patient treatment due to the intrinsic resistance characteristic of bacterial biofilms. This high biofilm production by invasive, multi-resistant staphylococci exacerbates the challenge [17].

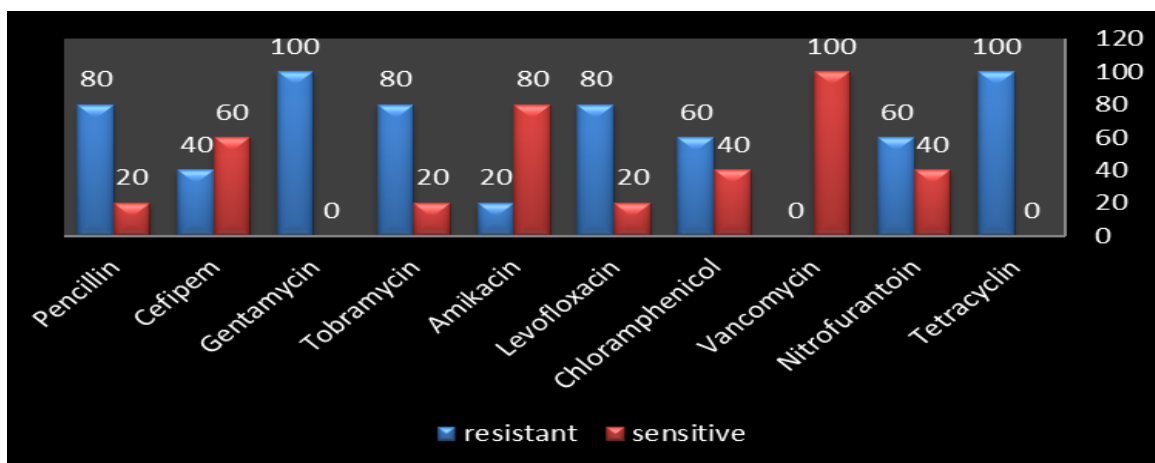


Figure 2 Staphylococcus aureus Susceptibility test.

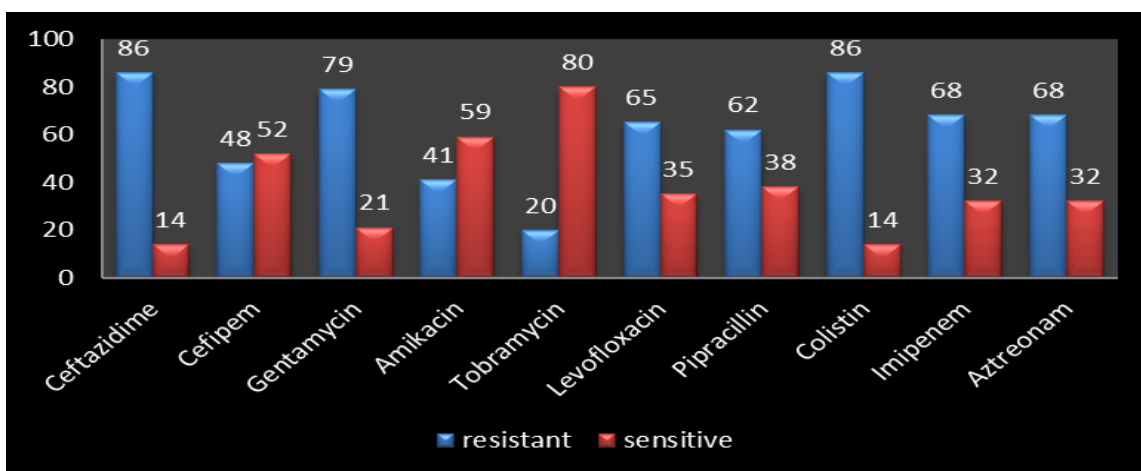


Figure 3 Susceptibility test of Klebsiella pneumonia.

3.3 Biofilm Formation

Using the traditional microtiter plate method, biofilm formation in *S. aureus* was categorized as follows: 20% exhibited weak biofilm formation, 30% moderate, and 50% strong, as illustrated in Figure 4. For *Klebsiella pneumoniae*, the distribution was 21% weak, 24% moderate, and 55% strong, depicted in Figure 5. The study of biofilm formation by clinical isolates underscores the significant role biofilms play in chronic infections. A comparison between antimicrobial resistance and biofilm production capabilities revealed that multidrug-resistant (MDR) phenotypes were more prevalent among biofilm-forming bacteria. This is evident in the characterization of biofilms produced by the multidrug-resistant *Klebsiella pneumoniae* strain from dental samples [18].

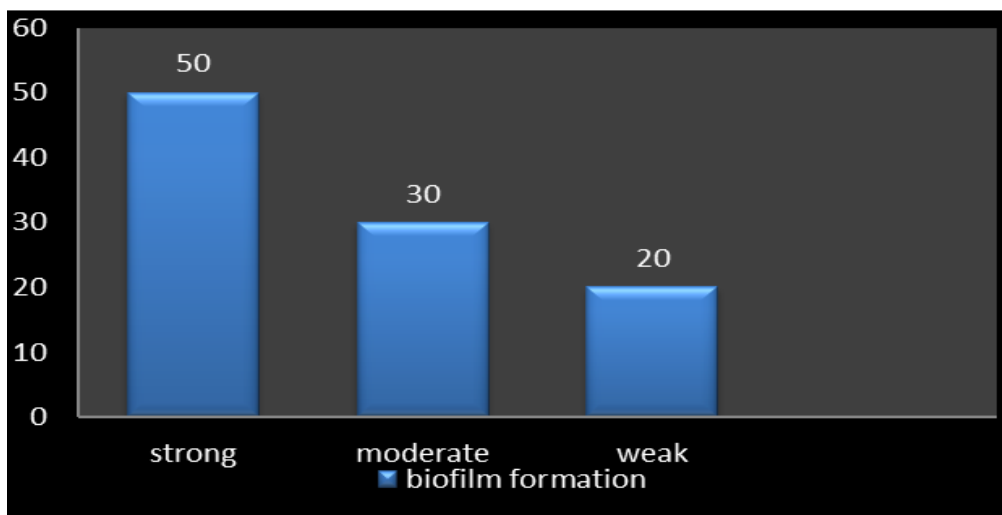


Figure 4 Staphylococcus aureus formation of Biofilm.

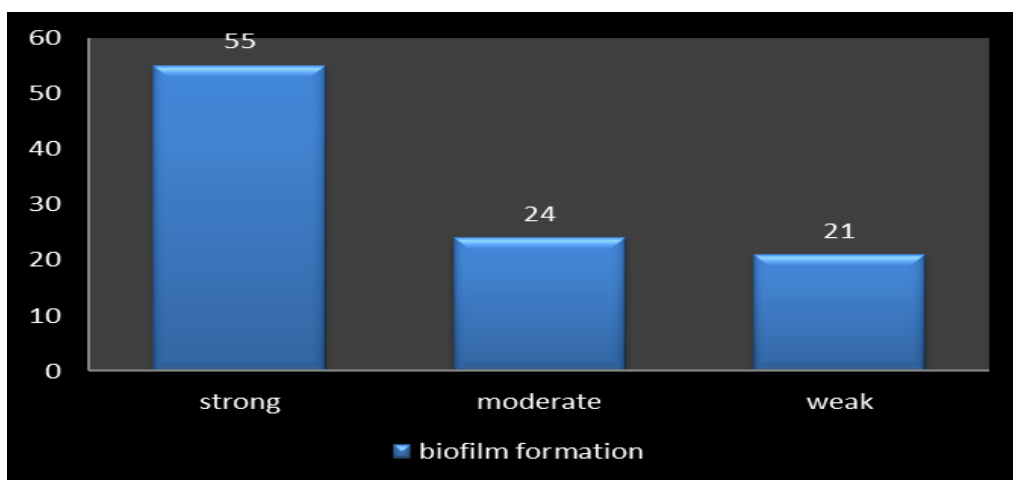


Figure 5 pseudomonas aeruginosa formation of Biofilm.

3.4 Chitosan Extraction

The traditional method for extracting commercial chitin from crustacean exoskeletons involves two key steps: (i) removing proteins using alkali treatment and (ii) extracting calcium carbonate and calcium phosphate through acidic treatment at elevated temperatures. Initially, shrimp shells undergo treatment with sodium hydroxide and Hydrochloride to remove proteins and minerals, effectively reducing nitrogen content by eliminating proteins and other nitrogenous substances. Chitin molecules, arranged in helicoidal microfibrillar structures within shell proteins, naturally bind to, minerals, lipids, proteins and pigments. However, aggressive acidic treatments can lead to polymer hydrolysis, resulting in variable chitin properties and environmental pollution. Furthermore, high NaOH concentrations and elevated temperatures during deproteinization can cause chitin deacetylation and depolymerization. To determine the optimal conditions and validate.

3.5 Chitosan Characterizations

3.5.1 Determination of Deacetylation Degree (DDA)

During the bioconversion process, the produced chitosan's degree of deacetylation (DDA) was evaluated. But only a meager yield (3.8 mg/g) was produced following a 5-day incubation period. Despite the characterization of the chitin deacetylase (CDA) enzyme, the insoluble structure of chitin makes it challenging to achieve a high degree of deacetylation. As a result, many techniques have been used to change the amorphous structure and decrease crystallinity of chitin in order to improve its qualities. These changes are essential to the proper access and conversion of chitin into chitosan by the CDA enzyme [19].

3.5.2 FTIR Spectroscopy

The FT-IR spectrum, was used to characterize and confirm the specific functional groups of the synthesized chitosan, which ranged from 400 to 4000 cm^{-1} . The IR spectra of the separated segments matched those of commercially produced chitosan made from shrimp shells. The FT-IR spectra, as displayed in Figure 6, indicate a large absorption band corresponding to hyd stretching vibrations between 3000 and 3500 cm^{-1} . Furthermore, the range of 1400–1650 cm^{-1} indicates the existence of C=O bonds. Approximately 2885 cm^{-1} (aliphatic C–H stretching), 1650 cm^{-1} , 1589 cm^{-1} (Amide II), 1326 cm^{-1} (Amide III), and 1080 cm^{-1} (C–O–C stretching vibrations) are some other notable peaks. The results of the IR spectra verify that the basic molecular structures of commercial and produced chitosan are very similar [20].

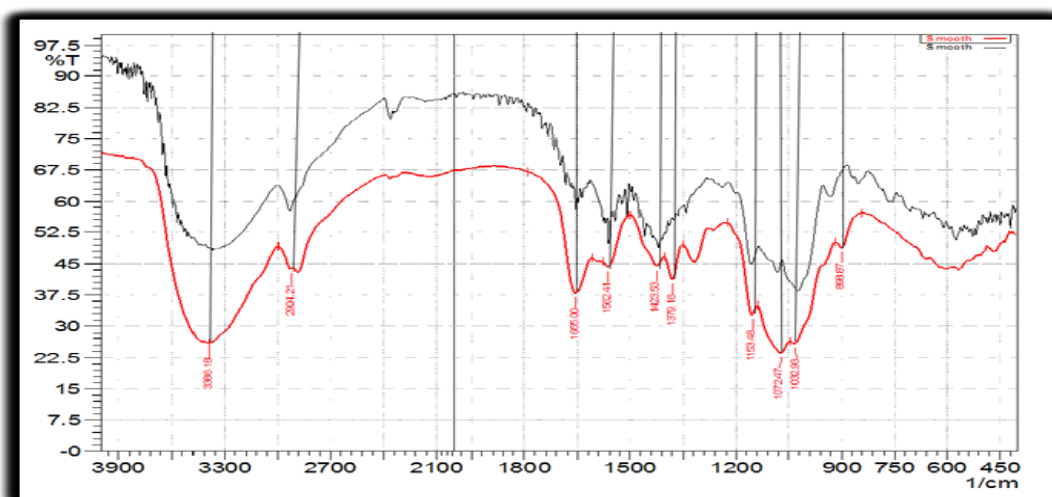


Figure 6 The FTIR spectra comparison shows commercial chitosan represented in red, while the chitosan produced by *Aspergillus flavus* F3 in solid-state fermentation (SSF) is depicted in black.

3.5.3. Chitosan's Anti-Biofilm Efficacy

Recent studies evaluated the biofilm development of *Klebsiella pneumoniae* and *Staphylococcus aureus* when exposed to chitosan at a minimum inhibitory concentration (MIC) of 1.6 mg/ml using a microtiter plate assay and crystal violet staining. Using an ELISA reader, the absorbance of the stained biofilms was determined at 590 nm. The findings showed that the anti-biofilm qualities of chitosan were sensitive to both *Staphylococcus aureus* and *Klebsiella pneumoniae*. In comparison to the control samples that

lacked chitosan, chitosan significantly reduced the production of biofilms at a concentration of 1.6 mg/ml. Figures 7 show how chitosan affects the formation of biofilms [22].

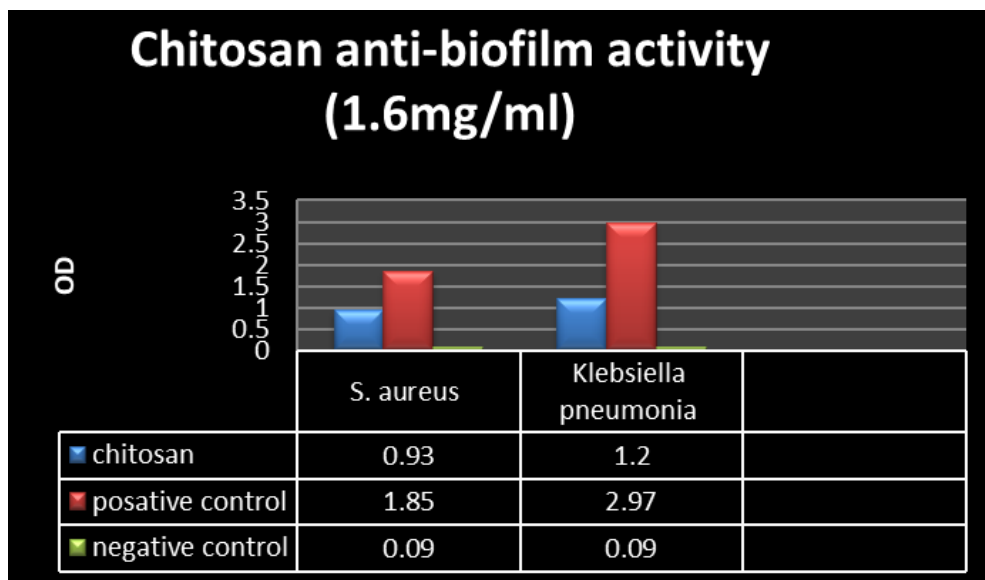


Figure 7 Chitosan's Anti-Biofilm Activity Against *S. aureus* and *K. pneumoniae*.

4. CONCLUSIONS

In conclusion, this study investigated the effect of chitosan on the biofilm-forming capacity of clinically isolated bacteria, particularly *Staphylococcus aureus* and *Klebsiella pneumoniae*. Chitosan, a biopolymer derived from chitin, was tested at various concentrations. The study included 136 clinical burn swap samples from patients at Medical City Hospital, with 19 samples testing positive for *Staphylococcus aureus* and 70 samples for *Klebsiella pneumoniae*. Of these, five *Staphylococcus aureus* and twenty-five *Klebsiella pneumoniae* strains were found to form biofilms when cultivated in microtiter plates. The results demonstrated that chitosan was effective in inhibiting biofilm formation, particularly at a dosage of 1.6 mg/ml. These findings suggest that chitosan could potentially be used to combat multidrug-resistant bacteria (MDR) in the future. Further research is warranted to explore the full therapeutic potential of chitosan in preventing biofilm formation and treating MDR infections.

References

- [1] M.E. Abd El-Hack, M.T. El-Saadony, M.E. Shafi, N.M. Zabermawi, *Int. J. Biol. Macromol.* 164 (2020) 2726
- [2] F.Z. Aboudamia, M. Kharroubi, M. Neffa, F. Aatab, S. Hanoune, M. Bouchdoug, A. Jaouad, *J. Air Waste Manag. Assoc.* 70 (2020) 118
- [3] K. Sauer, et al., *Dev. Biofilm* (2002) 1140
- [4] S.C. Davis, et al., *Wound Repair Regen.* 16 (2008) 23
- [5] B. Bendjemil, M. Mechi, K. Safi, M. Ferhi, K. Horchani Naifer, *Exp. Theo. NANOTECHNOLOGY* 8 (2024) 51
- [6] A.M.A. Alwaise, R.H. Rajab, A.A. Mahmood, M.A. Alreshedi, *Exp. Theo. NANOTECHNOLOGY* 8 (2024) 67
- [7] R.M. Donlan, J.W. Costerton, *Clin. Microbiol. Rev.* 15 (2002) 167

- [8] E. Garza-Gonzalez, R. Morfin-Otero, M.A. Martinez-Vazquez, E. Gonzalez-Diaz, O. Gonzalez-Santiago, E. Rodriguez-Noriega, *Scand. J. Infect. Dis.* 43 (2011) 930
- [9] C.-L. Ke, et al., *Polymers* 13 (2021) 904
- [10] R. Barbour, Sage (2013)
- [11] L.W. Auerbach, S.L. Goodbred Jr., D.R. Mondal, C.A. Wilson, K.R. Ahmed, K. Roy, B.A. Ackerly, *Nature Clim. Change* 5 (2015) 153
- [12] H. Lade, J.-S. Kim, *Antibiotics* 10 (2021) 398
- [13] X. Wu, D.A. Al Farraj, J.R. Rajaselvam, R.M. Alkufeidy, P. Vijayaraghavan, N.A. Alkubaisi, P. Agastian, M.K. Alshammari, *Saudi J. Biol. Sci.* 27 (2020) 2955
- [14] H.H. Liou, M.C. Tsai, C.J. Chen, J.S. Jeng, Y.C. Chang, S.Y. Chen, R.C. Chen, *Neurology* 48 (1997) 1583
- [15] M. Beaney, *The Analytic Turn: Analysis in Early Analytic Philosophy and Phenomenology* (2007) 1
- [16] C. Chatterjee, M. Paul, L. Xie, W.A. Van Der Donk, *Chem. Rev.* 105 (2005) 633
- [17] R.P. Schuenck, S.A. Nouér, C. Winter, et al., *J. Antimicrob. Chemother.* 74 (2019) 3122
- [18] A.S. Shon, R.P.S. Bajwa, T.A. Russo, *Virulence* 4 (2013) 107
- [19] CLSI, *Clin. Lab. Stand. Inst.* (2020)
- [20] J.H. Merritt, D.E. Kadouri, G.A. O'Toole, *Curr. Protoc. Microbiol.* 1B.1.1-1B.1.18 (2005)
- [21] R.A.A. Muzzarelli, *Carbohydr. Polym.* 35 (1997) 273
- [22] M.N.V. Ravi Kumar, *React. Funct. Polym.* 46 (2000) 1